Applied Science and Engineering Progress, Vol. 20, No. 3, 2027, 8319

Research Article

Impacts of Silicon Fertilization on Phytolith Accumulation and Morphological Variation in Rice

Ratchapon Prakongkaew, Attachai Trunjaruen, and Wasinee Pongprayoon*
Department of Biology, Faculty of Science, Burapha University, Chonburi, Thailand

Chakkree Lekklar
Division of Agricultural Technology, Faculty of Science and Technology, Rajabhat Rajanagarindra University, Chachoengsao, Thailand

Boonlue Kachenchart
Faculty of Environment and Resource Studies, Mahidol University, Nakhon Pathom, Thailand

Marsuton Sanyapeung
Pathum Thani Rice Research Center, Division of Rice Research and Development, Department of Rice, Pathum Thani, Thailand

Prapakorn Tantayotai
Department of Microbiology, Faculty of Science, Srinakharinwirot University, Bangkok, Thailand

* Corresponding author. E-mail: wasinee@buu.ac.th DOI: 10.14416/j.asep.2026.09.010
Received: 22 June 2026; Revised: 6 August 2026; Accepted: 21 August 2026; Published online: 16 September 2026

Abstract
Phytoliths are microscopic silica bodies formed within plant tissues and deposited in intercellular and intracellular spaces, contributing to long-term soil fertility and carbon sequestration. However, the effects of different silicon fertilizer sources on phytolith accumulation and morphology in rice remain unclear. Therefore, this study aimed to compare monosilicic acid and sodium metasilicate in terms of their effects on phytolith accumulation, physiological responses, phytolith morphology, and soil phytolith composition in RD43 rice. Sodium metasilicate application increased shoot phytolith content and chlorophyll b concentration. It also significantly enhanced the electron transport rate (ETR), tiller number, and root length. A total of 15 phytolith morphotypes were identified across fertilized and unfertilized treatments. Bilobate was the most common phytolith type in both roots and shoots. Bulliform flabellate and spheroidal psilate were observed only in the shoots of rice treated with sodium metasilicate. Four silica-containing mineral phases—quartz, alum, halloysite, and kaolinite–montmorillonite—were identified in the soil phytolith fractions. Quartz and alum were more abundant in the soil treated with sodium metasilicate. These findings suggest that the type of silicon fertilizer may influence phytolith distribution and accumulation in plants, as well as the mineral composition of soil phytolith fractions. Sodium metasilicate shows potential as an effective silicon source with both agronomic and environmental benefits.

Keywords: Carbon sequestration, Monosilicic acid, Phytolith, Rice Silicon, Sodium metasilicate

1 Introduction

Phytoliths are silica structures from amorphous biogenic silica ($SiO_2 \cdot nH_2O$) that accumulate in living plant tissues during growth and development [1]. Their formation and stability depend on factors such as pH, taxon, and weathering processes. Phytoliths play significant biological roles by contributing to plant resistance to biotic and abiotic stresses. Phytoliths are also widely applied in taxonomy, archeology, and paleoclimate reconstruction [2]. More recently, researchers have employed phytoliths to investigate the origin, development, and spread of agriculture. They are typically well preserved in soils and sediments after plant decomposition and can persist for millions of years under diverse climatic and environmental

Applied Science and Engineering Progress, Vol. 20, No. 3, 2027, 8319

conditions [3]. Phytoliths are produced by a wide range of plant species, particularly grasses such as rice (*Oryza sativa*), wheat (*Triticum aestivum*), maize (*Zea mays*), and bamboo species. Their morphology varies significantly among species and across different plant parts [3]. Phytolith grain size generally ranges from 20 to 200 μm, with a specific gravity of 2.1–2.3 [4]. Phytolith concentrations in plants range from 50 to 150 g kg^{-1} [5], whereas phytoliths generally constitute up to 30% of total soil mass [6]. In plants, roots actively absorb silicon from soil, taking up as much as 90% and transporting it to the shoots [7]. After translocation, silicic acid becomes concentrated and passively polymerized into amorphous silica (phytolith) at concentrations >2 mmol L^{-1}. In contrast, monosilicic acid concentrations in soil are ≤2 mmol L^{-1}; therefore, polymerization occurs primarily within plants [7]. Phytoliths typically assume the shape of the cells in which they are deposited and are not further mobilized or translocated. Phytoliths consist of approximately 66–91% silicon dioxide (SiO_2) [8], [9]. Phytoliths contribute to the preservation of soil organic carbon and mitigate carbon loss to the atmosphere by enhancing soil stability and limiting erosion. Their low susceptibility to microbial degradation and oxidation reduces the likelihood of carbon dioxide (CO_2) release into the atmosphere. Consequently, this carbon remains stable and is stored in soil for extended periods [10]. The persistence of phytoliths in plant detritus and soil strata represents a significant mechanism for carbon sequestration.

Rice is a staple food for the majority of the global population, and its cultivation is a major agricultural activity worldwide [11]. However, it contributes significantly to greenhouse gas emissions. The anaerobic conditions in flooded rice paddies favor methane (CH_4) production, a greenhouse gas that contributes to global warming [12]. Rice cultivation emits approximately 25–100 million metric tons of methane annually, accounting for 10%–12% of global methane emissions. This variability reflects differences in farming practices, water management, rice cultivars, soil properties and composition, and climatic conditions [11]. Harvesting removes a substantial amount of silicon from paddy fields, making it difficult to maintain soil silicon balance through natural weathering alone [5], [13].

In rice cultivation, silica fertilization can enhance plant growth and structural strength. Silicon fertilizers, including silicon dioxide, silicic acid, and sodium metasilicate, increase the concentration of soluble silica in soil, which is readily absorbed by plant roots [14]. A field study on rice cultivation assessed the impact of three silicon sources—diatomaceous earth, silicic acid, and rice husk biochar—on phytolith production, plant carbon content, and soil properties [9]. Silicon fertilization promotes the uptake of soluble silicon by roots and increases phytolith production in plant tissues [15]. A meta-analysis of over 3,500 data points from 87 studies revealed that paddy soils in major rice-producing regions are often deficient in silicon. Silicon fertilization increased rice yield by an average of 36% and biomass by 39% [16]. However, it remains unclear whether different silicon fertilizer sources differ in their effectiveness for phytolith accumulation, phytolith morphological expression, and soil phytolith dynamics under comparable cultivation conditions. Therefore, this study employed a pot experiment to compare the effects of two silicon fertilizer sources on phytolith accumulation, physiological indices, phytolith morphology, and soil phytolith composition in RD43 rice. Given the agronomic and environmental challenges associated with rice cultivation, identifying a practical and cost-effective silicon source is essential for sustainable agricultural management.

2 Material and methods

2.1 *Plant materials, growing conditions, and experiment design*

Seeds of RD43 rice (*O. sativa* L. spp. *indica*) were obtained from the Pathum Thani Rice Research Center (Thailand). Seeds were germinated for 2 weeks and transplanted into plastic pots containing 12 kg of soil. Silicon fertilizers were applied as monosilicic acid (H_4SiO_4) or sodium metasilicate (Na_2SiO_3) at 0.33 g kg^{-1} soil, while untreated pots served as controls. Soil properties were pH 6.52, organic matter 4.01%, total N 0.22%, available P 14.20 mg kg^{-1}, exchangeable K 57.20 mg kg^{-1}, and SiO_2 0.02% [17]-[19]. Plants were grown under greenhouse conditions (32 ± 2°C day, 28 ± 2°C night, 16 h light/8 h dark) in a completely randomized design with three biological replicates.

2.2 *Sample collection and preparation*

Plants and soil were collected at the flowering stage (60 days after planting). Four plants per biological replicate were harvested for physiological assessment. The plants were rinsed twice with distilled water and separated into shoots (leaf sheath, stem, and leaf

blade) and roots. Soil from rice cultivation was dried in a hot-air oven at 70°C for 24 h to obtain a constant dry weight before phytolith analysis.

2.3 *Plant and soil phytolith contents*

Phytoliths from root and shoot tissues were extracted using the dry-ash method described by Parr *et al.,* [20]. Dried samples were ashed at 500°C and subsequently treated with HCl and H_2O_2 to remove carbonates and organic matter before phytolith recovery. Soil phytoliths were extracted following the modified wet oxidation method of Zuo *et al.,* [21]. Samples were treated with Calgon solution, H_2O_2, and HCl, followed by density separation using $ZnBr_2$ (2.35 g mL^{-1}). The recovered phytolith fraction was dried and weighed.

2.4. *Physiological measurements*

Chlorophyll a, chlorophyll b, and total chlorophyll contents were determined according to Shabala *et al.,* [22] and Lichtenthaler [23]. Chlorophyll fluorescence parameters (Fv/Fm, ΦPSII, and ETR) were measured using standard fluorometric methods. Tiller number and root length were recorded for growth assessment.

2.5 *Rice phytolith morphology and soil phytolith composition*

Extracted phytoliths were mounted on microscope slides and examined under an optical microscope (400×). Morphotypes were identified according to the International Code for Phytolith Nomenclature 2.0 [24]. Soil phytolith composition was analyzed by X-ray diffraction (XRD; SmartLab, Rigaku, USA). Mineral phases were identified from characteristic diffraction peaks, and relative abundances were estimated using the SmartLab software package.

2.6 *Principal component analysis, Pearson correlation, and statistical analysis*

Principal component analysis (PCA) was conducted using the SRplot platform to identify data clustering and variance [25]. Pearson correlation analysis was performed to assess relationships among variables, and the results were visualized using the "corrplot" package in R program version 0.92 [26]. Phytolith content and physiological data were analyzed using analysis of variance (ANOVA), followed by Tukey's test for mean comparison, with statistical significance set at p-value < 0.05. All analyses were performed using Minitab 18.0 (Minitab Inc., Coventry, UK). Error bars in all figures represent the standard deviation of the mean.

3 Results and Discussion

3.1 *Rice phytolith content and physiological response to silicon fertilizer application*

Silicon fertilizer increased phytolith concentration in rice plants. Numerical increases in root phytolith (RP) content were observed under monosilicic acid and sodium metasilicate treatments. However, these differences were not statistically significant compared with the control (Figure 1a). In contrast, sodium metasilicate significantly increased shoot phytolith (LP) content (3.0 ± 0.02%), representing 1.3- and 2.1-fold increases compared with the control and monosilicic acid treatments, respectively (Figure 1b).

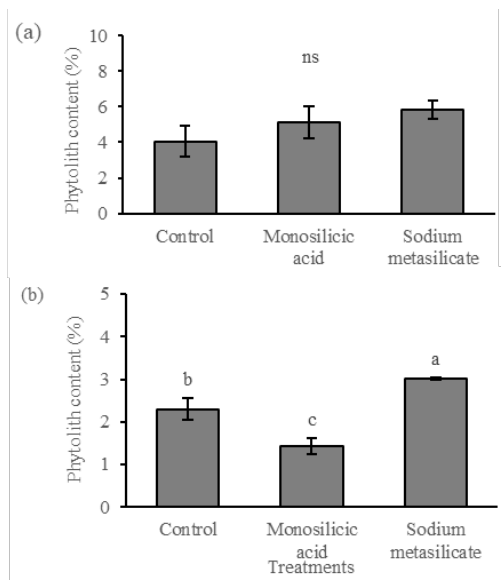

Figure 1: Phytolith contents in (a) root and (b) shoot of rice genotypes subjected to silicon fertilization (monosilicic acid and sodium metasilicate) and without silicon fertilization (control). Data are presented as mean ± SD, derived from three independent replicates. Different lowercase letters indicate significant differences, p-value < 0.05, ANOVA followed by Tukey's test. Ns is not significant.

Applied Science and Engineering Progress, Vol. 20, No. 3, 2027, 8319

The effects of silicon fertilization on photosynthetic and growth parameters were also investigated. Sodium metasilicate increased chlorophyll *b* (Chl *b*) content (141.7 ± 43.50 µg g^{-1} of fresh weight) compared with the control (86.6 ± 19.83 µg g^{-1} fresh weight), representing a 1.6-fold increase. In contrast, chlorophyll a (Chl *a*) and total chlorophyll (Chl *a* + Chl *b*) remained unchanged across treatments (Figures 2a–c). Photosynthetic efficiency parameters in shoots showed that sodium metasilicate increased Maximum quantum efficiency of photosystem II (Fv/Fm) by 1.0-fold compared with monosilicic acid. It also increased quantum efficiency in light (ΦPSII) by 1.3-fold relative to monosilicic acid. Electron transport rate (ETR) (243 ± 52.9 $mmol^{-1}$ m^{-2} s^{-1}) was significantly higher in the sodium metasilicate-treated plants, with a 1.9-fold significant increase relative to the control (Figures 2d–f). Growth parameters were also enhanced under the sodium metasilicate treatment. Tiller number (6.3 ± 1.24) and root length (38.0 ± 9.89 cm) increased significantly by 1.3- and 1.7-fold, respectively, compared with the control (Figures 2g–h).

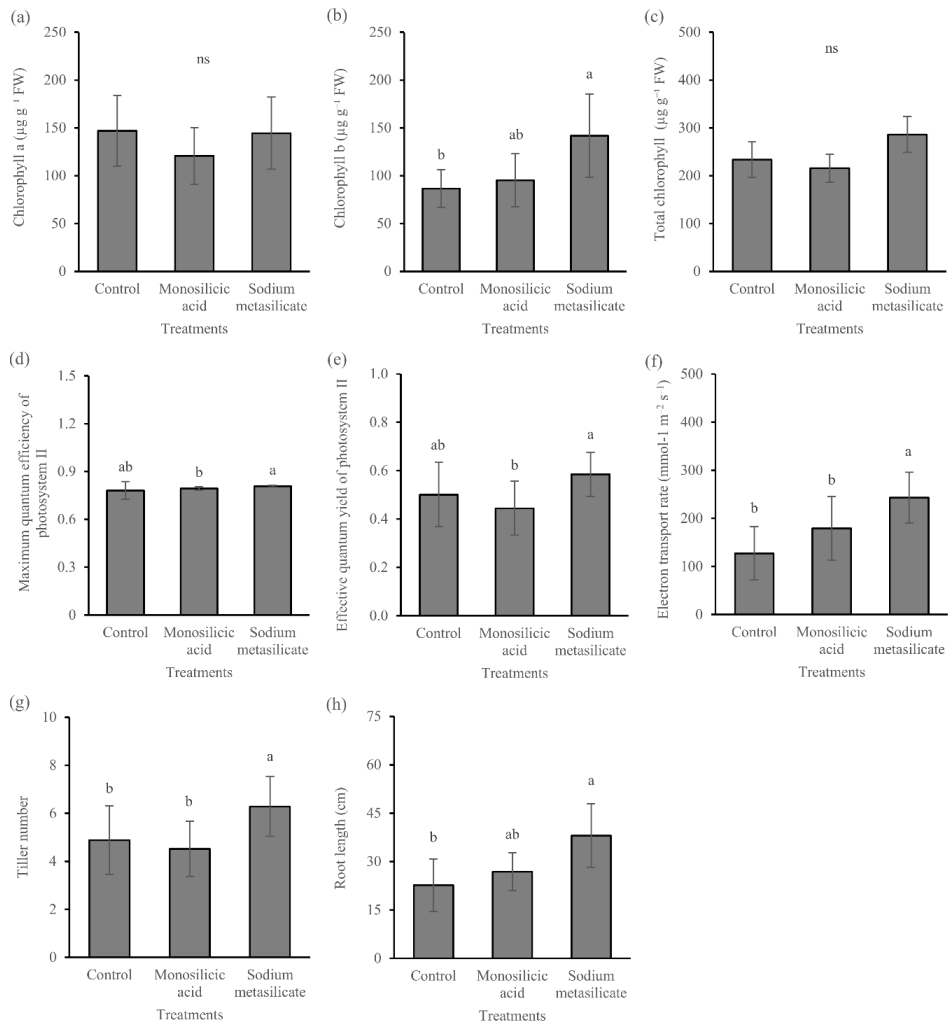

Figure 2: Physiological indices, including (a) chlorophyll a (Chl *a*), (b) chlorophyll b (Chl *b*), (c) total chlorophyll (Chl *a* + Chl *b*), (d) Maximum quantum efficiency of photosystem II (Fv/Fm), (e) quantum efficiency in light (ΦPSII), (f) electron transport rate (ETR), (g) tiller number, and (h) root length under silicon fertilization (monosilicic acid and sodium metasilicate) and without silicon fertilization (control).

3.2. *Correlation and grouping of plant phytolith content and physiological attributes*

Pearson's correlation analysis of phytolith content and physiological parameters in roots and shoots, with and without silicon fertilization, is shown in Figure 3a. Variables included RP, LP, Chl *a*, Chl *b*, total chlorophyll (TotalChl), Fv/Fm, ΦPSII, ETR, tiller number (Tillering), and root length (RL). RP showed a significant positive correlation with ETR (r = 0.65). However, no significant correlation was observed between RP and LP (r = 0.39). LP was positively correlated with Fv/Fm (r = 0.65) and ΦPSII (r = 0.63). Chl *a*, Chl *b*, and TotalChl were positively correlated with ΦPSII (r = 0.77, 0.79, and 0.87), Tillering (r = 0.61, 0.78, and 0.74), and RL (r = 0.54, 0.88, and 0.74). Fv/Fm was positively correlated with ΦPSII (r = 0.77). Both ΦPSII and ETR showed positive correlations with Tillering (r = 0.73 and 0.84) and RL (r = 0.81 and 0.95). Tillering was strongly correlated with RL (r = 0.95). PCA revealed a clear separation between silicon-treated and control groups based on phytolith and physiological parameters. PC1 and PC2 explained 62.9% and 19.9% of the total variance, respectively. As shown in Figure 3b, silicon fertilization distinctly separated treatment groups from the control.

3.3 *Rice phytolith morphology in root and shoot*

A total of 15 phytolith morphotypes were identified in roots and shoots under both silicon-fertilized and control conditions (Table 1; Figure 4). Six morphotypes were observed in roots: acute bulbosus, bilobate, bulliform flabellate, elongate entire, polygonal, and polyhedral. Nine morphotypes were identified in shoots: acute bulbosus, bilobate, blocky, bulliform flabellate, elongate dentate, elongate entire, scutiform, spheroidal psilate, and trapezoid. Across all treatments, polygonal and polyhedral were unique to roots, whereas blocky, elongate dentate, scutiform, spheroidal psilate, and trapezoid were unique to shoots. Four morphotypes—bilobate, elongate entire, bulliform flabellate, and acute bulbosus—were common to both roots and shoots (Table 1). In roots, bilobate and elongate entire phytoliths were consistently observed across all treatments (Figures 4a, c, k, l, r, and s). The polygonal and polyhedral types were detected only in the control (Figures 4d–e). Acute bulbosus was observed only under monosilicic acid treatment (Figure 4j). In shoots, bilobate remained the predominant morphotype (Figures 4f, n, and u). The elongate dentate and trapezoid types were unique to the control (Figures 4h–i). Acute bulbosus and scutiform were specific to the monosilicic acid treatment (Figures 4m, q), whereas bulliform flabellate and spheroidal psilate were observed only under sodium metasilicate treatment (Figures 4w, x).

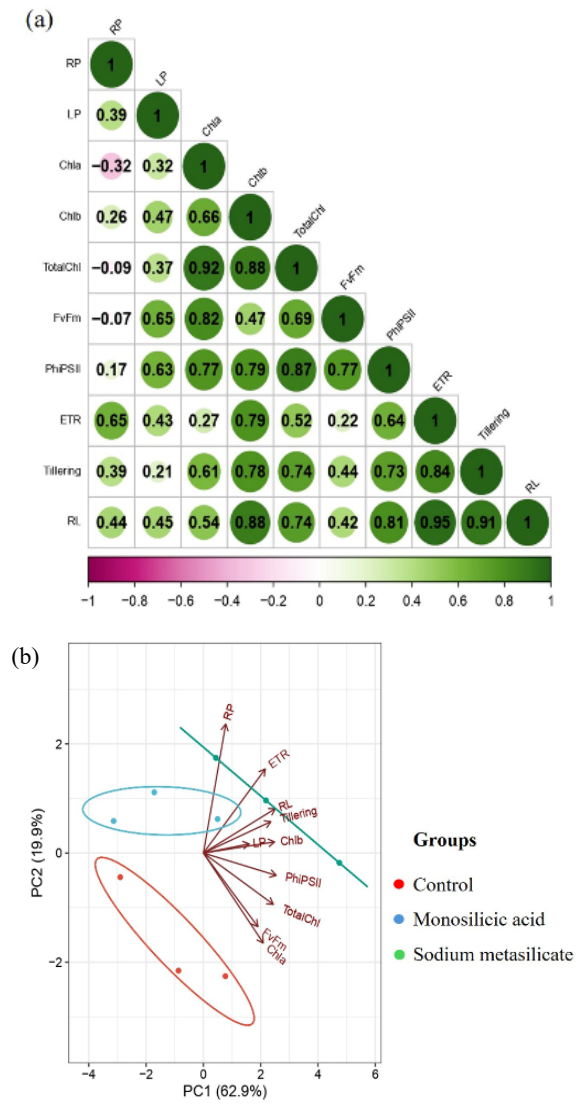

Figure 3: (a) Pearson correlation and (b) principal component analysis (PCA) plot of rice phytolith and physiological parameter data obtained from applications with and without silica fertilizer. Root phytolith (RP), shoot phytolith (LP), Chl *a*, Chl *b,* TotalChl, Fv/Fm, ΦPSII, ETR, tiller number (Tillering), and root length (RL).

Applied Science and Engineering Progress, Vol. 20, No. 3, 2027, 8319

Table 1: Phytolith morphotypes identified in roots and shoots under silicon fertilization and control conditions.

Phytolith morphotypes	C	M	S	Figures
Root				
Acute bulbosus	−	+	−	4j
Bilobate	+	+	+	4a, 4k, and 4r
Bulliform flabellate	+	−	+	4b and 4t
Elongate entire	+	+	+	4c, 4l, and 4s
Polygonal	+	−	−	4d
Polyhedral	+	−	−	4e
Shoot				
Acute bulbosus	−	+	−	4m
Bilobate	+	+	+	4f, 4n, and 4u
Blocky	+	+	−	4g and 4o
Bulliform flabellate	−	−	+	4w
Elongate dentate	+	−	−	4h
Elongate entire	−	+	+	4p and 4v
Scutiform	−	+	−	4q
Spheroidal psilate	−	−	+	4x
Trapezoid	+	−	−	4i

C, control; M, monosilicic acid; S, sodium metasilicate; (+), presence of phytolith morphotype; (−), absence of phytolith morphotype

3.4 *Soil phytolith concentration and composition under silicon fertilizer supply*

Soil phytolith content showed an inverse trend relative to plant phytolith concentration. Phytolith content in sodium metasilicate-treated soil (0.6%) was significantly lower than in the control (1.4%) (Figure 5a). To further assess the effects of silicon fertilization, soil phytolith composition was analyzed. Four silica derivatives—quartz, alum, halloysite, and kaolinite–montmorillonite—were identified. Quartz and alum were more abundant in sodium metasilicate-treated soil, increasing by 2.2- and 1.3-fold, respectively, compared with the control (Figures 5b–c). Conversely, halloysite (8.7%) and kaolinite–montmorillonite (32.3%) were lower under sodium metasilicate treatment, decreasing by 2.6- and 1.2-fold, respectively. Monosilicic acid treatment resultedin the highest abundance of kaolinite–montmorillonite (44.3%) in soil phytoliths (Figures 5d–e).

4 Discussion

4.1 *Sodium metasilicate-induced phytolith accumulation in shoots through roots and changes in physiological indices*

This study evaluated the effects of two silicon fertilizer sources, monosilicic acid and sodium metasilicate, on phytolith accumulation and physiological responses in rice under greenhouse pot conditions. Silicon fertilizers are inorganic sources that increase the availability of plant-available silicon in soil, primarily in the form of monosilicic acid. This increase reflects the dissolution and release dynamics of silicate fertilizers in lowland rice ecosystems. This increase in available silicon is likely due to the addition of silicate materials, which contribute to soluble silicon pools. Under submerged conditions, the concentration of monosilicic acid in soil solution increases following silicate fertilizer application, facilitating the formation of polysilicic acids [27].

During the pot experiment, flooded soil amended with sodium metasilicate likely provided sustained silicon release, enhancing its availability as a nutrient source. Sodium metasilicate showed greater potential as a silicon source than monosilicic acid. In agricultural soils, silicon is the second most abundant element (>50% SiO_2), its plant-available form (monosilicic acid) is typically low. Silicon predominantly occurs in crystalline forms, such as silicate minerals, secondary clays, and quartz, which limit its availability to plants [28]. Dissolved silicon released from highly soluble sodium metasilicate significantly contributes to the pool of bioavailable silicon, which is absorbed by roots and translocated to shoots through the xylem during transpiration [29]. Silicon fertilizers are absorbed by roots and subsequently deposited as phytoliths in plant tissues [1]. The greater effectiveness of sodium metasilicate may be attributed to its higher solubility under flooded conditions, which continuously replenishes the pool of plant-available silicon [27]. Because silicon absorbed by roots is subsequently transported through

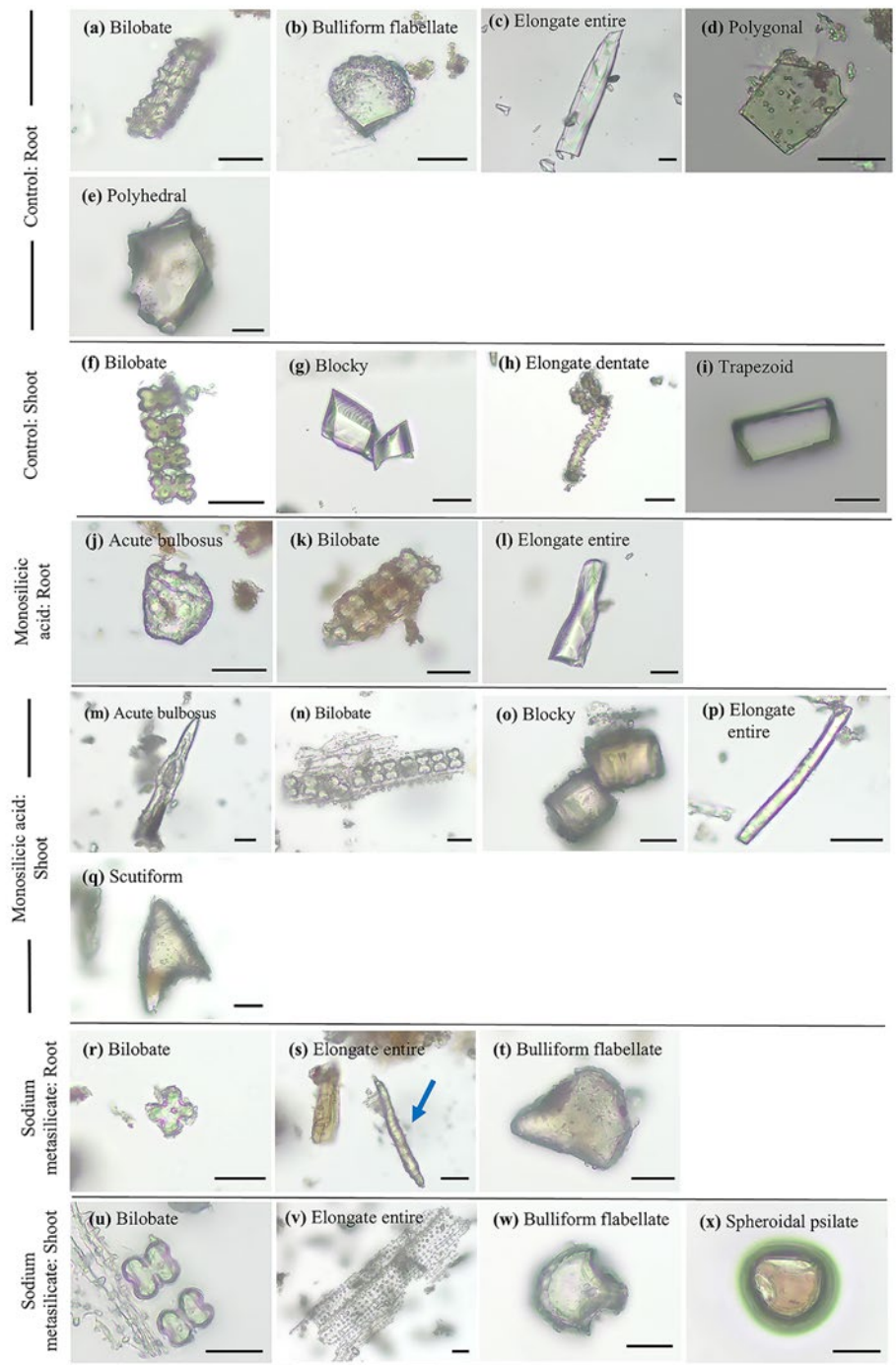

Figure 4: Phytolith morphologies under control group in (a-e) roots and (f-i) shoots. Phytolith morphologies under monosilicic acid treatment in roots (j-l) and shoots (m-q). Phytolith morphologies under sodium metasilicate treatment in (r-t) roots and (u-x) shoots were detected in rice. Bar = 20 µm.

Applied Science and Engineering Progress, Vol. 20, No. 3, 2027, 8319

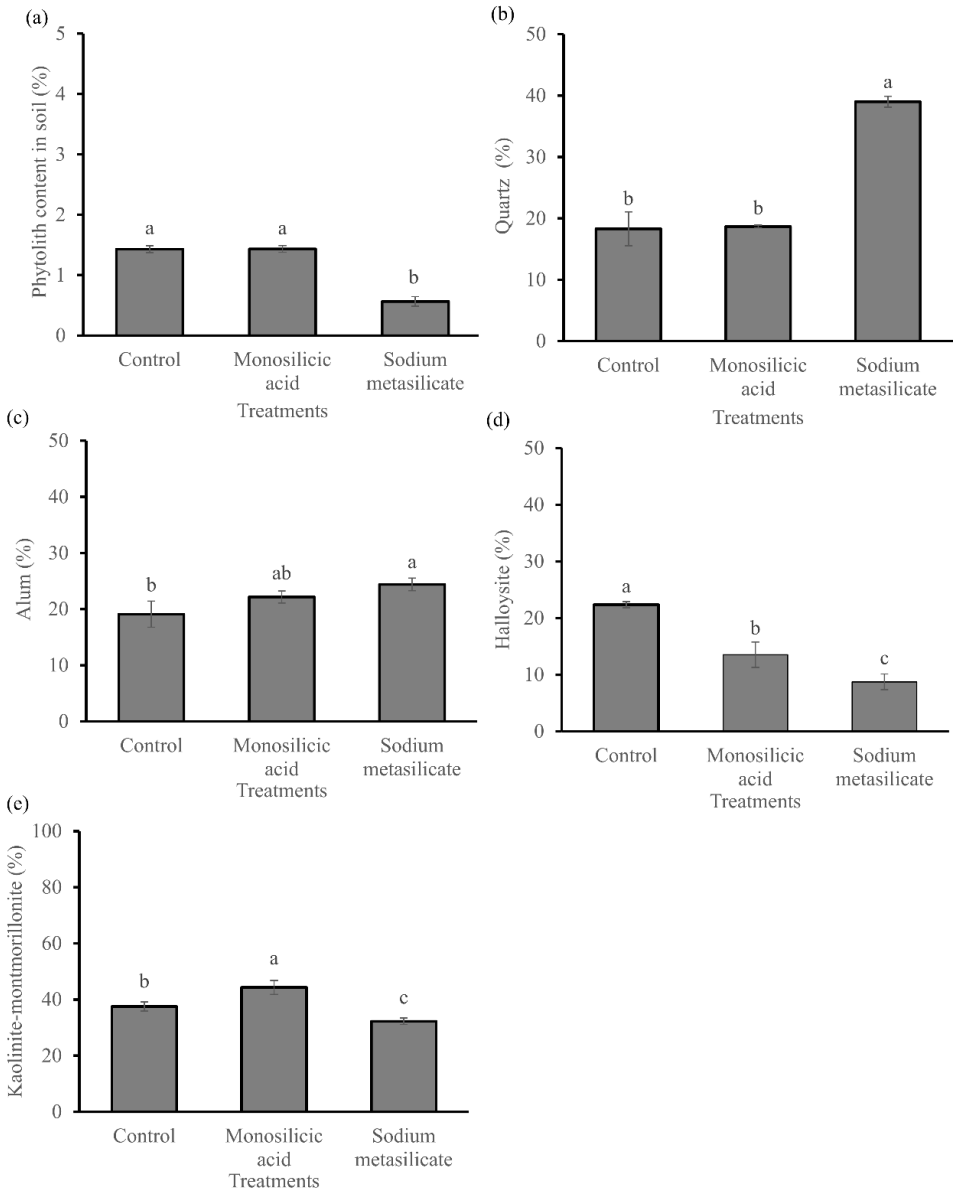

Figure 5: (a) Phytolith contents were detected in soil. Soil phytolith composition, namely (b) quartz, (c) alum, (d) halloysite, and (e) kaolinite-montmorillonite under with and without silicon fertilization. Quartz, SiO_2; alum-Na, $NaAl(SO_4)_2(H_2O)_{12}$; halloysite, $Al_2Si_2O_5(OH)_4$; kaolinite-montmorillonite, $Na_{0.3}Al_4Si_6O_{15}(OH)_6 \cdot 4H_2O$.

above-ground tissues, enhanced silicon availability may have contrib uted to the greater phytolith accumulation observed in shoots than in roots, potentially explaining why significant increases were detected in shoot phytolith content but not in root phytolith content [30]. In the present study, sodium metasilicate increased phytolith content in roots and significantly enhanced accumulation in shoots (Figure 1). Although root phytolith content increased numerically following silicon fertilization, no significant differences were observed among treatments. Because roots serve as the primary site of silicon uptake and transport, greater phytolith accumulation in shoots may reflect the continued

translocation and deposition of translocated silicon from root tissues [7], [29]. Furthermore, no significant correlation was observed between RP and LP (r = 0.39), suggesting that root phytolith accumulation alone may not directly determine phytolith deposition in shoots (Figure 3a).

Rice is a silicon-accumulating species with tissue concentrations of 10–15%, of which approximately 90% is deposited as phytoliths. A significant correlation has been reported between silicon fertilization and phytolith accumulation across rice organs, including shoots (stem, leaf sheath, and leaf blade) and roots [5]. The results indicated that sodium metasilicate treatment produced the highest Chl *b* content and enhanced chlorophyll fluorescence parameters (Fv/Fm, phiPSII, and ETR) (Figure 2). These parameters were positively associated with plant growth, including tiller number and RL (Figure 3a). Meunier *et al.,* [31] reported that silicon uptake by roots promotes phytolith accumulation in plant tissues, thereby enhancing photosynthetic efficiency. Similarly, silicon uptake improves leaf photosynthetic performance and increases biomass production in grass [15]. Silicon application increases rice root growth by 20%–30% [10]. In addition to facilitating silicic acid transport to above-ground organs, root cells accumulate silicon, especially in cell walls, similar to leaf cells. In rice roots, silicon promotes suberin deposition and tissue lignification. Moreover, total silicon content is often higher in roots than in the above-ground organs [32].

4.2 *Rice phytolith morphological variation under silicon fertilization in roots and shoots*

Phytolith morphology varied across rice organs. Based on their formation mechanism, available silicon in soil is absorbed by roots and deposited within plant cells, where phytoliths assume the shape of the cell or cell sap [5]. The results identified both common and unique phytolith morphotypes in roots and shoots across all treatments, with and without silicon fertilization (Table 1; Figure 4). Bilobate and elongate entire were consistently observed in roots across all treatments, while bilobate was also consistently present in shoots. Bilobate (dumbbell-shaped) phytoliths, a key morphotype in grasses, were consistently observed and are widely regarded as diagnostic silica bodies. Variation in lobate morphology has been linked to environmental conditions, especially moisture. Hygrophytic grasses typically produce lobate phytoliths with short shanks, whereas xerophytic grasses produce lobate phytoliths with long shanks [33]. Following silicon fertilization with monosilicic acid, acute bulbosus phytoliths were abundant in both roots and shoots (Table 1; Figures 4j, m). These structures are typically formed from fully silicified epidermal hair cells [34]. Similar phytoliths have been reported in the leaves of *Rostraria cristata* (Poaceae) [2] and in the culm sheath of bamboo (*D. brandisii*) [35]. Furthermore, sodium metasilicate treatment increased the occurrence of bulliform flabellate and spheroidal phytoliths in leaves (Figures 4w, x). In *Oryza*, bulliform phytoliths typically exhibit a fan-shaped morphology with scale-like ornamentation on the rounded surface. These large, specialized epidermal cells are arranged in longitudinal rows within leaf furrows in Poaceae. The surface outlines reflect impressions of adjacent cells [24].

Previous studies have used the size and morphology of bulliform flabellate phytoliths to distinguish rice and compare wild and domesticated varieties [36], [37]. Spheroidal psilate phytoliths were also detected in shoots under sodium metasilicate treatment (Figure 4x). This morphotype is commonly reported in leaves and is considered to originate from epidermal or subepidermal tissues [3]. Spheroidal psilate phytoliths are characterized as solid or hollow bodies with a spheroidal to slightly ellipsoidal or irregular shape, generally resembling a sphere. Their surfaces are smooth, without ornamentation or projections. These phytoliths often form as vesicular infillings of epidermal and parenchyma cells of foliage and reproductive organs across a wide range of dicots and monocots (e.g., Arecaceae, Poaceae, and Cyperaceae), as well as some gymnosperms [24]. Silicon fertilization did not appear to alter phytolith morphology (Table 1; Figure 4). Instead, it influenced the occurrence of specific morphotypes among treatments. This observation may reflect differences in tissue silicification and silicon deposition patterns associated with silicon availability [7], [30], [38].

4.3 *Effects of silicon fertilization on soil phytolith concentration and composition*

In the soil samples, sodium metasilicate application resulted in the lowest phytolith content (0.5% of soil dry weight) (Figure 5a). In contrast, this treatment

produced the highest phytolith accumulation in plants, reaching 5.8% and 3.0% of the plant dry weight in roots and shoots, respectively (Figure 1). This pattern suggests that sodium metasilicate may have promoted more efficient utilization of available silicon, resulting in greater phytolith deposition in rice tissues; however, silicon uptake was not directly measured in the present study [7], [29], [30]. This may be explained by the active uptake of silica from the soil during plant growth and its subsequent deposition within plant cells, resulting in a higher phytolith concentration in the shoot. Sodium metasilicate altered soil phytolith composition by increasing quartz and alum content, whereas monosilicic acid promoted kaolinite–montmorillonite. Halloysite content decreased under both silicon treatments (Figures 5b–e). Quartz, halloysite, kaolinite, and alum are key components of soil silica that influence silicon availability for plant uptake and phytolith formation [38]. Unlike crystalline silica forms, such as quartz, phytolith silica is amorphous (opal-A). Quartz does not form phytolith structures. However, it can coexist with phytoliths in soil, reflecting a silica-rich environment from which plants draw their nutrients. Quartz is a primary source of silica during weathering, whereas clay minerals such as halloysite and kaolinite, which are composed of aluminum silicates, release silica more gradually. Alum influences soil pH and nutrient dynamics, thereby indirectly affecting silicon availability [39]. Overall, sodium metasilicate altered soil phytolith composition and was associated with lower soil phytolith content but greater phytolith accumulation in rice tissues. These findings suggest more efficient utilization of available silicon under the experimental conditions.

5 Conclusions

This study demonstrated that silicon fertilization influenced phytolith accumulation, physiological responses, phytolith morphotype occurrence, and soil phytolith composition in RD43 rice. Among the two silicon sources evaluated, sodium metasilicate was more effective than monosilicic acid in enhancing shoot phytolith accumulation, chlorophyll *b* content, electron transport rate, tiller number, and root length. Treatment-specific phytolith morphotypes were also observed under different silicon sources. Furthermore, sodium metasilicate altered soil phytolith composition and may promote more efficient silicon utilization by rice plants. Future research should investigate silicon uptake mechanisms and validate these findings under field conditions to support sustainable rice production and phytolith-occulated carbon sequestration.

Acknowledgments

The authors are grateful to the Biology Department, Faculty of Science, Burapha University, for providing laboratory facilities. We thank Ms. Kamolnat Thongchai and Ms. Papakkanan Rotjanakiet for laboratory assistance. The authors would like to thank Enago (www.enago.com) for the English language editing. This research was financially supported by (i) Burapha University (BUU), (ii) Thailand Science Research and Innovation (TSRI), and (iii) National Science Research and Innovation Fund (NSRF) (Fundamental Fund: Grant no. 2.27/2568). This work was also partially supported by a Full-time Researcher Fellowship Award from Burapha University (PostGrad 2568/04).

Author Contributions

R.P.: investigation, methodology, data analysis; A.T.: data analysis; C.L.: investigation, data analysis; B.K.: conceptualization, research design, data analysis; M.S.: methodology; P.T.: data analysis; W.P.: conceptualization, data curation, writing—reviewing and editing, funding acquisition, project administration. All authors have read and agreed to the published version of the manuscript.

Conflicts of Interest

The authors declare no conflict of interest.

Declaration of generative AI and AI-assisted technologies in the writing process

The authors utilized the ChatGPT tool to enhance the language and readability of the manuscript.

References

[1] Z. Li, F. Guo, J.-T. Cornelis, Z. Song, X. Wang, and B. Delvaux, “Combined silicon-phosphorus fertilization affects the biomass and phytolith stock of rice plants,” *Frontiers in Plant Science*,vol. 11, Art. no. 67, Feb. 2020, doi: 10.3389/fpls.2020.00067.

[2] P. Chowdhary, P. Badgal, M. A. Bhat, S. A. Shakoor, B. A. Mir, and A. S. Soodan, "Phytoliths analysis in root, culm, leaf and synflorescence of *Rostraria cristata* (Poaceae)," *Journal of Plant Research*, vol. 136, pp. 787-801, Aug. 2023, doi: 10.1007/s10265-023-01485-1.

[3] X. An and B. Xie, "Phytoliths from woody plants: A review," *Diversity*, vol. 14, no. 5, Art. no. 339, Apr. 2022, doi: 10.3390/d14050339.

[4] W. Chen, "A review on diagnostic phytoliths for the application in paleovegetation reconstruction and environmental archaeology in East Asia," *International Journal of Geosciences*, vol. 15, no. 6, pp. 479-492, Jun. 2024, doi: 10.4236/ijg.2024.156026.

[5] X. Sun, Q. Liu, T. Tang, X. Chen, and X. Luo, "Silicon fertilizer application promotes phytolith accumulation in rice plants," *Frontiers in Plant Science*, vol. 10, Art. no. 425, Apr. 2019, doi: 10.3389/fpls.2019.00425.

[6] X. Sun, Q. Liu, J. Gu, X. Chen, and K. Zhu, "Evaluation of the occluded carbon within husk phytoliths of 35 rice cultivars," *Frontiers of Earth Science*, vol. 10, no. 4, pp. 683-690, Dec. 2016, doi: 10.1007/s11707-015-0549-9.

[7] R. Mandlik et al., "Significance of silicon uptake, transport, and deposition in plants," *Journal of Experimental Botany*, vol. 71, no. 21, pp. 6703-6718, Dec. 2020, doi: 10.1093/jxb/eraa301.

[8] M. Anjum and N. B. Prakash, "Production of phytolith and PhytOC and distribution of extractable Si pools in aerobic rice as influenced by different Si sources," *Frontiers in Plant Science*, vol. 14, Art. no. 1146416, Aug. 2023, doi: 10.3389/fpls.2023.1146416.

[9] M. Anjum and P. B. Nagabovanalli, "Assessing production of phytolith and phytolith occluded carbon in above-ground biomass of intensively cultivated rice ecosystems in India," *Carbon Management*, vol. 12, no. 1, pp. 509-519, Sep. 2021, doi: 10.1080/17583004.2021.1978552.

[10] R. Xu, J. Huang, H. Guo, C. Wang, and H. Zhan, "Functions of silicon and phytolith in higher plants," *Plant Signaling & Behavior*, vol. 18, no. 1, Art. no. 2198848, Dec. 2023, doi: 10.1080/15592324.2023.2198848.

[11] A. Ahmad, M. Zoli, C. Latella, and J. Bacenetti, "Rice cultivation and processing: Highlights from a life cycle thinking perspective," *Science of the Total Environment*, vol. 871, Art. no. 162079, May 2023, doi: 10.1016/j.scitotenv.2023.162079.

[12] M. SaberiKamarposhti, K.-W. Ng, M. Yadollahi, H. Kamyab, J. Cheng, and M. Khorami, "Cultivating a sustainable future in the artificial intelligence era: A comprehensive assessment of greenhouse gas emissions and removals in agriculture," *Environmental Research*, vol. 250, Art. no. 118528, Jun. 2024, doi: 10.1016/j.envres.2024.118528.

[13] N. K. Savant, G. H. Snyder, and L. E. Datnoff, "Silicon management and sustainable rice production," in *Advances in Agronomy*, vol. 58, D. L. Sparks, Ed., San Diego, CA, USA: Academic Press, 1996, pp. 151-199, doi: 10.1016/S0065-2113(08)60255-2.

[14] W. Pan, L. Zhang, F. Li, X. Wang, and Y. Liu, "Silica nanoparticle accumulation in plants: Current state and future perspectives," *Nanoscale*, vol. 15, no. 37, pp. 15079-15091, Sep. 2023, doi: 10.1039/D3NR02221H.

[15] I. U. Rehman and I. Rashid, "Role of silicon in phytolith-occluded carbon (PhytOC) sequestration," *Vegetos*, vol. 37, no. 4, pp. 1221-1231, Dec. 2024, doi: 10.1007/s42535-023-00659-5.

[16] X. Yang et al., "Silicon in paddy fields: Benefits for rice production and the potential of rice phytoliths for biogeochemical carbon sequestration," *Science of the Total Environment*, vol. 929, Art. no. 172497, Jun. 2024, doi: 10.1016/j.scitotenv.2024.172497.

[17] D. W. Nelson and L. E. Sommers, "Total carbon, organic carbon, and organic matter," in *Methods of Soil Analysis, Part 2: Chemical and Microbiological Properties*, 2nd ed., A. L. Page, R. H. Miller, and D. R. Keeney, Eds. Madison, WI, USA: American Society of Agronomy and Soil Science Society of America, 1982, pp. 539-579. doi: 10.2134/agronmonogr9.2.2ed.c29.

[18] J. M. Bremner and C. S. Mulvaney, "Nitrogen-Total," in *Methods of Soil Analysis, Part 2: Chemical and Microbiological Properties*, 2nd ed., A. L. Page, R. H. Miller, and D. R. Keeney, Eds. Madison, WI, USA: American Society of Agronomy and Soil Science Society of America, 1982, pp. 595-624. doi: 10.2134/agronmonogr9.2.2ed.c31.

[19] R. H. Bray and L. T. Kurtz "Determination of total, organic, and available forms of phosphorus in soils," *Soil Science*, vol. 59, no. 1,

pp. 39–46, Jan. 1945, doi: 10.1097/00010694-194501000-00006.

[20] J. F. Parr, V. Dolic, G. Lancaster, and W. E. Boyd, "A microwave digestion method for the extraction of phytoliths from herbarium specimens," *Review of Palaeobotany and Palynology*, vol. 116, no. 3-4, pp. 203-212, Sep. 2001, doi: 10.1016/S0034-6667(01)00089-6.

[21] X. Zuo, H. Lu, and Z. Gu, "Distribution of soil phytolith-occluded carbon in the Chinese Loess Plateau and its implications for silica–carbon cycles," *Plant and Soil*, vol. 374, no. 1-2, pp. 223-232, Jan. 2014, doi: 10.1007/s11104-013-1850-6.

[22] S. N. Shabala, S. I. Shabala, A. I. Martynenko, O. Babourina, and I. A. Newman, "Salinity effect on bioelectric activity, growth, Na+ accumulation and chlorophyll fluorescence of maize leaves: A comparative survey and prospects for screening," *Australian Journal of Plant Physiology*, vol. 25, no. 5, pp. 607–616, Aug. 1998, doi: 10.1071/PP97146.

[23] H. K. Lichtenthaler, "Chlorophylls and carotenoids: Pigments of photosynthetic biomembranes," in *Methods in Enzymology*, vol. 148, L. Packer and R. Douce, Eds. San Diego, CA, USA: Academic Press, 1987, pp. 350-382, doi: 10.1016/0076-6879(87)48036-1.

[24] International Committee for Phytolith Taxonomy (ICPT), "International code for phytolith nomenclature (ICPN) 2.0," *Annals of Botany*, vol. 124, no. 2, pp. 189-199, Jul. 2019, doi: 10.1093/aob/mcz064.

[25] D. Tang, M. Chen, X. Huang, and G. Zhang, "SRplot: A free online platform for data visualization and graphing," *PLoS ONE*, vol. 18, no. 11, Art. no. e0294236, Nov. 2023, doi: 10.1371/journal.pone.0294236.

[26] T. Wei and V. Simko, "R package 'corrplot': Visualization of a correlation matrix," version 0.92, 2021. [Online]. Available: https://github.com/taiyun/corrplot.

[27] J. K. Malav et al., "Rice yield and available nutrients status of loamy sand soil as influenced by different levels of silicon and nitrogen," *International Journal of Current Microbiology and Applied Sciences*, vol. 7, no. 2, pp. 619–632, Feb. 2018, doi: 10.20546/ijcmas.2018.702.077.

[28] I. U. Rehman, M. A. Malik, I. Rashid, I. A. Sheergojri, and R. A. Dar, "Silicon fertilization increases carbon sequestration by augmenting PhytOC production in wheat," *Journal of Soil Science and Plant Nutrition*, vol. 23, no. 1, pp. 696-706, Mar. 2023, doi: 10.1007/s42729-022-01110-5.

[29] N. Chaiwong and C. Prom-u-thai, "Significant roles of silicon for improving crop productivity and factors affecting silicon uptake and accumulation in rice: A review," *Journal of Soil Science and Plant Nutrition*, vol. 22, no. 2, pp. 1970-1982, Feb. 2022, doi: 10.1007/s42729-022-00787-y.

[30] S. Huang and J. F. Ma, "Silicon transport and its 'homeostasis' in rice," *Quantitative Plant Biology*, vol. 5, Art. no. e20, Jan. 2024, doi: 10.1017/qpb.2024.19.

[31] J. D. Meunier, A. Alexandre, M. Maschia, S. Borschneck, and F. Torrence, "Effect of phytoliths for mitigating water stress in durum wheat," *New Phytologist*, vol. 215, no. 1, pp. 229-239, Jul. 2017, doi: 10.1111/nph.14554.

[32] O. Nedukha, "Tolerance of plant cell wall to environment," in *Advances in Plant Defense Mechanisms*, London, U.K.: IntechOpen, Jun. 2022, doi: 10.5772/intechopen.105452.

[33] H. Lu and K.-B. Liu, "Morphological variations of lobate phytoliths from grasses in China and the southeastern United States," *Diversity and Distributions*, vol. 9, no. 1, pp. 73-87, Jan. 2003, doi: 10.1046/j.1472-4642.2003.00166.x.

[34] T. An, J. Chen, Y. Zheng, S. Huo, and W. Gu, "Morphometric distinction between Acute bulbosus phytoliths (silicified epidermal hair cells) from *Panicum miliaceum* and *Setaria italica* leaves," *Vegetation History and Archaeobotany*, vol. 33, pp. 629-641, Jun. 2024, doi: 10.1007/s00334-024-00999-5.

[35] S. Duan, X. Li, Y. Yang, L. Zhang, and H. Chen, "Silicon deposition and phytolith morphological variation in culm sheaths of *Dendrocalamus brandisii* at different growth stages," *Plants*, vol. 14, no. 6, Art. no. 841, Mar. 2025, doi: 10.3390/plants14060841.

[36] D. M. Pearsall, D. R. Piperno, E. H. Dinan, M. Umlauf, Z. Zhao, and R. A. Benfer, "Distinguishing rice (*Oryza sativa* Poaceae) from wild *Oryza* species through phytolith analysis: Results of preliminary research," *Economic Botany*, vol. 49, no. 2, pp. 183-196, Apr. 1995, doi: 10.1007/BF02862923.

[37] X. Huan, H. Lu, C. Wang, X. Zhang, and C. Ge, "Bulliform phytolith research in wild and

domesticated rice paddy soil in South China," *PLoS ONE*, vol. 10, no. 10, Art. no. e0141255, Oct. 2015, doi: 10.1371/journal.pone.0141255.

[38] N. Zexer, S. Kumar, and R. Elbaum, "Silica deposition in plants: Scaffolding the mineralization," *Annals of Botany*, vol. 131, no. 6, pp. 897-909, May 2023, doi: 10.1093/aob/mcad044.

[39] E. Durgut, M. Cinar, M. Terzi, I. Kursun Unver, Y. Yildirim, and O. Ozdemir, "Evaluation of different dispersants on the dispersion/sedimentation behavior of halloysite, kaolinite, and quartz suspensions in the enrichment of halloysite ore by mechanical dispersion," *Minerals*, vol. 12, no. 11, Art. no. 1426, Nov. 2022, doi: 10.3390/min12111426.